NYS000520
Submitted: June 9, 2015
Proceedings of PVP2014
2014 ASME Pressure Vessels and Piping Division Conference
July 20-24, 2014, Anaheim, CA, USA

PVP2014-28540

ASSESSMENT OF FRACTURE TOUGHNESS MODELS FOR FERRITIC STEELS USED IN SECTION XI OF THE ASME CODE RELATIVE TO CURRENT DATA-BASED MODELS

Mark Kirk[1]
Senior Materials Engineer, Nuclear Regulatory Commission, Rockville, MD, USA, mark.kirk@nrc.gov

Marjorie Erickson
President, Phoenix Engineering Associates, Inc. Unity, NH, USA, erickson@peaiconsulting.com

William Server
President, ATI Consulting, Black Mountain, NC, USA, wserver@ati-consulting.com

Gary Stevens[1]
Senior Materials Engineer, Nuclear Regulatory Commission, Rockville, MD, USA, gary.stevens@nrc.gov

Russell Cipolla
Principal Engineer, Intertek AIM, Sunnyvale, CA, USA, russell.cipolla@intertek.com

ABSTRACT

Section XI of the ASME Code provides models of the fracture toughness of ferritic steel. Recent efforts have been made to incorporate new information, such as the Code Cases that use the Master Curve, but the fracture toughness models in Section XI have, for the most part, remained unchanged since the K_{Ic} and K_{Ia} curves were first developed in Welding Research Council Bulletin 175 in 1972. Since 1972, considerable advancements to the state of knowledge, both theoretical and practical have occurred, particularly with regard to the amount of available data. For example, as part of the U.S. Nuclear Regulatory Commission's (NRC's) pressurized thermal shock (PTS) re-evaluation efforts the NRC and the industry jointly developed an integrated model that predicts the mean trends and scatter of the fracture toughness of ferritic steels throughout the temperature range from the lower shelf to the upper shelf. This collection of models was used by the NRC to establish the index temperature screening limits adopted in the Alternate PTS Rule documented in Title 10 to the U.S. Code of Federal Regulations (CFR), Part 50.61a (10CFR50.61a). In this paper the predictions of the toughness models used by the ASME Code are compared with these newer models (that are based on considerably more data) to identify areas where the ASME Code could be improved. Such improvements include the following:

- On the lower shelf, the low-temperature asymptote of the K_{Ic} curve does not represent a lower bound to all available data.
- On the upper shelf, the *de facto* K_{Ic} limit of applicability of 220 MPa√m exceeds available data, especially after consideration of irradiation effects.
- The separation between the K_{Ic} and K_{Ia} curves depends on the amount of irradiation embrittlement, a functionality not captured by the ASME Section XI equations.
- The temperature above which upper shelf behavior can be expected depends on the amount of irradiation embrittlement, a functionality not captured in the ASME Section XI equations.

BACKGROUND AND OBJECTIVE

A key input to assessments of the integrity of operating structures in the presence of real or postulated defects is the fracture toughness of the material in question. Various parts of the ASME Code (that is, the Code itself, various Nonmandatory Appendices, and Code Cases) provide models of the fracture toughness properties of ferritic steels; principally the K_{Ic} and K_{Ia} curves developed in the early 1970s [1]. The Code has recently been expanded to include procedures to estimate RT_{NDT} using the Master Curve index temperature T_o [2-3], and to estimate the temperature above which an EPFM-based analysis is needed [4]. Since the early 1970s, considerable advancements to the state of knowledge, both theoretical and practical have occurred, particularly with regard to the amount of data available and empirical models derived from these data. For example, as part of the U.S. Nuclear Regulatory Commission's (NRC's) pressurized thermal shock (PTS) re-evaluation efforts, reports from which were issued in early 2010, the NRC and the industry jointly developed an integrated model that predicts the mean trends and scatter of the fracture toughness of ferritic steels throughout the complete temperature range from the lower shelf to the upper shelf [5]. This collection of models was used by the NRC in the probabilistic fracture mechanics (PFM) Code, Fracture Analysis Vessels – Oak Ridge (FAVOR) [6], to establish the index temperature screening limits adopted in the Alternate PTS Rule

[1] The views expressed herein are those of these authors and do not represent an official position of the NRC. This material is the work of the United States Government and is not subject to copyright protection in the United States. This paper is approved for public release with unlimited distribution.

documented in Title 10 to the U.S. Code of Federal Regulations (CFR), Part 50.61a (10CFR50.61a) [7].

The objective of this paper is to compare the predictions of the toughness models within the ASME Code with the newer models that are based on considerably more data to identify areas where the ASME Code could be improved.

ASME CODE TOUGHNESS MODELS

The K_{Ic} and K_{Ia} curves that appear in Article A-4200 of Nonmandatory Appendix A to ASME Section XI [8] (the K_{Ic} curve also appears in Appendix G [9]), are expressed as follows (all equations in this paper are expressed in SI units):

$$K_{Ic} = 36.5 + 22.738 \times exp[0.036(T - RT_{NDT})] \quad (1)$$

$$K_{Ia} = 29.4 + 13.675 \times exp[0.0261(T - RT_{NDT})] \quad (2)$$

Eqs. (1-2) are intended to represent the lower bounds of K_{Ic} and K_{Ia} data. These estimates of K_{Ic} and K_{Ia} depend on the index temperature RT_{NDT}, which is determined per ASME NB-2331 [10]. Where appropriate, RT_{NDT} is adjusted to account for the effects of neutron irradiation embrittlement. Neither Appendix A nor Appendix G, place an upper-limit on the K_{Ic} value that may be estimates using eqs. (1-2). Nevertheless, a value of 220 MPa√m has, over time, become a *de facto* limit on K_{Ic} despite scarce mention or defense of this value in the literature. The basis for this limit and an assessment of its accuracy relative to data appears in [11].

CURRENT DATA-BASED TOUGHNESS MODELS

In 1984 Wallin and co-workers began publication of a series of papers that, collectively, describe what has come to be called the "Master Curve" [12-14]. The Master Curve quantifies the temperature dependence and scatter of the fracture toughness (i.e., K_{Jc} or J_c values) of ferritic steels in the fracture mode transition temperature region. Existing work in which large databases were examined demonstrates that the temperature dependence and scatter of the Master Curve are consistent for all ferritic steels [15-16][2]. All that needs to be determined for a particular material is the Master Curve index temperature (T_o), which positions the Master Curve on the temperature axis. Using ASTM E1921 protocols it is possible to estimate T_o using as few as six fracture toughness specimens [19], providing the possibility that T_o can be directly determined from the specimens already placed in the surveillance capsules of nuclear reactor pressure vessels.

Over the past fifteen years papers have been published that expand upon and extend the Master Curve concept. These papers describe:

- The temperature dependence and scatter in crack arrest fracture toughness (K_{Ia}) [20].
- The temperature separation of the K_{Jc} and K_{Ia} transition curves, and how this separation changes with the condition of the material [20-21]
- The temperature dependence and scatter in upper shelf fracture toughness data (J_{Ic}) [22-23], and
- The relationship between transition fracture toughness and upper shelf fracture toughness values [24].

References [4, 5, 20-24] discuss both the empirical and physical bases for these relationships, which were developed from large databases (data numbering in the hundreds) covering a wide range of material conditions (e.g., different product forms, different irradiation exposures, different material chemistries). These papers provide information demonstrating that, like the Master Curve, these relationships can be expected to apply with comparable accuracy to all ferritic steels irrespective of composition, product form, heat treatment, degree of hardening, degree of irradiation damage, etc. **Significantly, *all* of these models are linked via a single parameter: T_o.** Once T_o is determined the mean initiation and arrest toughness behavior, and the scatter about the mean, can be determined from lower shelf through upper shelf using combinations of the models presented in Table 1. Figure 1 shows the curve shapes and relationships of these models and defines their variables visually.

In addition to the models shown in Figure 1, Table 1 includes the equation for RT_{To} provided by Code Cases N-629 and N-631 (and now in the ASME Code Section XI, Appendices A and G). RT_{To} provides an alternative to RT_{NDT} such that T_o can be used to index the ASME K_{Ic} and K_{Ia} lower bound curves. RT_{To} thereby links the data-based models of Table 1 to the ASME models for K_{Ic} and K_{Ia}. This linkage enables comparison of the ASME lower bound descriptions of transition initiation and arrest toughness to the data-based models of initiation and arrest toughness.

COMPARISON OF ASME MODELS TO CURRENT DATA-BASED MODELS

The data-based models of ferritic steel toughness summarized in Table 1 can be compared with the ASME models for K_{Ic} and K_{Ia} to identify situations where the ASME models adequately reflect the data versus situations where the ASME models could potentially be improved. In the next two subsections [A and B] the comparisons made can be interpreted in two ways: (1) either as an assessment of the accuracy of the ASME models when RT_{To} (i.e., T_o) is used as an index temperature, or (2) as an assessment of the accuracy of the ASME models when the index temperature RT_{NDT} is used and RT_{NDT} exceeds T_o by ≈19.4 °C. Subsection C re-examines these analyses to assess the effect of the NDT/Charpy-based value of RT_{NDT} being other than ≈19.4 °C above T_o, which is often the case. Finally, an assessment is made in Subsection D of the influence margin terms have on the ability of the ASME models to represent, or conservatively bound, the fracture toughness data.

A. Crack Initiation – K_{Ic} and Upper Shelf

Figure 2 compares the predictions of the data-based models for K_{Ic} / K_{Jc} and J_{Ic} with the ASME K_{Ic} curve augmented by the *de facto* upper shelf limiting value of 220 MPa√m for three RT_{To} values: -100, 0, and +100 °C (these being chosen to examine a range of hardening that could result from, as an example, neutron radiation embrittlement). These graphs support the following observations:

- The ASME model over-estimates the lower shelf fracture toughness at temperatures ≈60 °C or more below RT_{To} for all values of RT_{To}. For un-irradiated materials such low temperatures cannot be achieved during normal operations. However, as radiation embrittlement causes the material transition temperature to approach regulatory limits (e.g., the PTS limits of 132 to 149 °C in 10CFR50.61 [25]) a temperature 60 °C below these values is clearly within the range achievable during a cool-down.

[2] Some studies by Wallin suggest adjustments to the Master Curve lower bound value on the lower shelf [17], and of the temperature dependence in the case of extremely high embrittlement [18]. In absolute terms the magnitude of these adjustments are minor, having only small effects on the predicted values. These adjustments could be considered as a further improvement to the models suggested herein should the cognizant ASME Code groups decide to adopt these models.

- In the transition regime between lower shelf and upper shelf the ASME model maintains a consistent location below the data, thus providing a conservative estimate of K_{Jc}. The well recognized difference between the temperature dependence of the data and that of the ASME model is also evident in these plots. While these differences could affect the outcome of probabilistic assessments, which are more sensitive to changes in the models near the lower bound, they are not expected to adversely affect deterministic assessments performed according to ASME SC-XI Appendix A or Appendix G.

Table 1. Summary of Data-Based Toughness Models for Ferritic Steels.

refs	Model		Equations	Eq. #
[2-3]	RT_{To}	Reference temperature for ASME K_{Ic} and K_{Ia} curves based on T_o	$RT_{NDT} \equiv RT_{To} = T_o + 19.4$	(3)
[12-14]	K_{Jc}	Temperature dependence of median fracture toughness of a 1T specimen	$K_{Jc} = 30 + 70 \cdot \exp(0.019(T - T_o))$	(4)
		Scatter at a fixed temperature	$K_{Jc}^{P_f} = K_{\min} + (K_o - 20)\left\{-\left[\ln(1-P_f)\right]^{1/4}\right\}$, where $K_o = 31 + 77 \cdot \exp(0.019(T - T_o))$	(5)
		Size effect	$K_{Jc(x)} = K_{\min} + \left(K_{Jc(o)} - K_{\min}\right)\left(\frac{B_o}{B_x}\right)^{1/b}$ where B_x is the thickness of the specimen of interest while B_o is the reference thickness (1-in., or 25.4 mm).	(6)
[20]	K_{Ia}	Temperature dependence of mean K_{Ia}	$K_{Ia} = 30 + 70 \cdot \exp(0.019(T - T_{KIa}))$	(7a)
		Scatter at a fixed temperature	Log-normal with a variance (σ) equal to 18% of the mean value.	(7b)
[22-23]	J_{Ic}	Temperature dependence (temperature is in Kelvin)	$J_{Ic} = 1.75\{C_1 \cdot \exp[-C_2 T_K + C_3 T_K \cdot \ln(\dot{\varepsilon})] - 3.325\} + J_{adj}$ $J_{adj} = J_{c(US)} - \Delta J_{Ic(US)}$ $J_{c(US)} = \{30 + 70 \cdot \exp(0.019(T_{US} - T_o))\}^2 (1 - \upsilon^2)/E$ $\Delta J_{Ic(US)} = 1.75\{C_1 \cdot \exp[-C_2 T_{US}^K + C_3 T_{US}^K \cdot \ln(\dot{\varepsilon})] - 3.325\}$ $E = \{207200 - 57.1 \cdot T\}$ $\nu = 0.3$ $T_{ref} = 288°C$ (or 561K) $T_{US}^K = T_{US} + 273.15$ $C_1 = 1033$ MPa $C_2 = 0.00698$/K $C_3 = 0.000415$/K $\dot{\varepsilon} = 0.0004$/sec	(8)
		Scatter at a fixed temperature	$\sigma_{\Delta J_{Ic}} = A \cdot e^{(B \cdot \hat{T})}$ where $\hat{T} = T - 288^\circ C$ $A = 9.03 \cdot e^{(1.12 \cdot P)}$ $B = MIN\{0, 0.0009P - 0.0045\}$ $P = MIN\{1, MAX[0, MIN(P_1, P_2)]\}$ $P_1 = \frac{J_{Ic(288)}}{120} - 0.46$ $P_2 = \frac{J_{Ic(288)}}{800} + 0.51$	(9)
[21, 34]	Linkage of K_{Jc} and K_{Ia} data		$T_{KIa} = T_o + 44.97 \times exp[-0.00613 \times T_o]$ The standard deviation of ln (T_{KIa}-T_o) is 0.383.	(10)
[24]	Linkage of K_{Jc} and J_{Ic} data		$T_{US} = 48.843 + 0.7985 T_o$	(11)

- The accuracy of the *de facto* ASME upper limit of 220 MPa√m on K_{Ic} is strongly compromised by increasing RT_{To} [11]. Above RT_{To} of 0 °C 220 MPa√m exceeds the upper shelf fracture toughness of most RPV steels by a considerable amount, suggesting a practical limit on K_{Ic} should be informed by the upper shelf fracture toughness. The upper shelf of many ferritic materials falls below 220 MPa√m even when $J_{0.1}$ is used as the characterizing parameter (see the Appendix for further discussion). T_{US}, defined in Table 1,

can be used to define the upper limit of applicability for the K_{Ic} curve based on data [11].[3]

B. Crack Arrest

Figure 3 compares the predictions of the data-based models for K_{Ic} / K_{Jc} and K_{Ia} with the ASME K_{Ic} and K_{Ia} curves for three RT_{To} values: -100, 0, and +100 °C (these being chosen to examine a range of hardening that could result from, as an example, neutron radiation embrittlement). The data-based models show that as RT_{To} increases the K_{Ic} and K_{Ia} curves converge. This convergence is not a feature of the ASME models, which maintain a constant temperature separation between them. The result of using a constant temperature separation to represent the actual material behavior is that the ASME model is overly pessimistic for high values of RT_{To} indicative of highly irradiated material and over-estimates K_{Ia} at low values of RT_{To}.

C. Sensitivity Study Based on the T_o - RT_{NDT} Relationship

As described in [2-3], RT_{To} was defined as T_o + 19.4 °C so that the K_{Ic} curve indexed to RT_{To} "appropriately bounds available fracture toughness data." "Appropriate" bounding was defined in [26] as a curve bounding approximately 95% of the data, a finding also validated by Wallin [27]. The consistent placement of the reference K_{Ic} curve enabled by the use of a true fracture toughness measure like T_o ensures that this degree of bounding will occur for all materials. Thus, the analysis of the previous section [B] applies to situations where RT_{To} is used as an index temperature, or to materials for which RT_{NDT} exceeds T_o by ≈19.4 °C. However, RT_{NDT} does not always equal T_o +19.4 °C. Figure 4 draws together data from two sources (one being the source used to establish the epistemic uncertainty in RT_{NDT} for the PFM computer code FAVOR [6]) to illustrate that the degree by which RT_{NDT} exceeds (or in one case does not) T_o varies by a considerable degree. The following values of (RT_{NDT} -T_o) were taken from these data and used to re-plot the ASME models in the format of Figure 2 and Figure 3 to assess the degree to which the ASME models represent the data for different values of RT_{NDT}:

- RT_{NDT} = T_o + 0 °C: This is an extreme case, but nonetheless possible based on these data and moreover is representative of a worst-case assessment of the conservatism of the ASME models.
- RT_{NDT} = T_o + 47 °C: This represents the median of the distribution of (RT_{NDT} -T_o) values shown on Figure 4.

Figure 5 illustrates that the deficiencies of the ASME K_{Ic} model in representing the lower shelf and upper limit of applicability noted in the discussion of Figure 2 are not influenced by the difference between RT_{NDT} and T_o. For materials where RT_{NDT} exceeds T_o by less than 19.4 °C, Figure 5 illustrates that non-conservative predictions of K_{Ic} in transition can also be expected.

Figure 6 illustrates that RT_{NDT} would need to exceed T_o by more than 47 °C (a value of approximately 65 °C would be needed) to ensure that the ASME K_{Ia} model provides a conservative bound to the K_{Ia} data for the range of RT_{To} values considered. The data in Figure 4 demonstrate that such materials make up only 25% of the population of RPV steels. Thus, the use of RT_{To} to index the K_{Ia} curve will provide a non-conservative representation for approximately 75% of RPV materials. Another paper presented at this conference [34] corrects this situation by using eq. (10) to adjust RT_{To} so that it can be used to index the K_{Ia} curve.

D. Effect of Margins

Taken as a whole, the information in subsections [A], [B], and [C] leads to the conclusion that the ASME models are out of date and, in some cases, non-conservative. Especially on the lower shelf, the upper transition limit, and for all of the crack arrest transition, the ASME models fail to capture trends clearly evident in data now available. Even the application of large margins implicit to some RT_{NDT} values does not fully ameliorate the non-conservatisms identified here (see Figure 4).

Table 2. ASME Code margin terms.

Code Ref.	Margin Values	Equation
Appendix G	2 for current practice	$K_I < 2K_{Im} + K_{It}$
	1 for risk informed	$K_I < 1K_{Im} + K_{It}$
IWB-3612/ Appendix A	√10 for normal and anticipated loading	$K_I < K_{Ic}/\sqrt{10}$
	√2 for emergency and faulted loading	$K_I < K_{Ic}/\sqrt{2}$

In view of these observations, the question arises as to how the ASME Code models survived for over 40 years without these inaccuracies becoming evident. The primary explanation is the margins placed on loading, flaw size, and the effects of radiation embrittlement. The deterministic method described in the ASME Code, Appendix G, uses these margins with the expectation that they account for these discrepancies between the data and the ASME models..Some of the specific margins applied are listed below:

- Margin on irradiated RT_{NDT}: The ASME Code states that RT_{NDT} should be adjusted to account for the effects of radiation damage. Regulatory Guide 1.99 Revision 2 suggests a margin term that accounts for uncertainty in the unirradiated value of RT_{NDT} and in the estimated shift of this value due to irradiation damage [29]. The value for each of these terms depends on several factors (e.g., product form, generic or measured values, credibility of surveillance data, etc.). To provide a sense of the magnitude of the margin term the range of values adopted for the various materials in the operating fleet reported in the NRC's RVID2 database is provided in Figure 7 [30].
- Margin on K_I: Table 2 summarizes some of the different margins applied to the value of K_I in different parts of the ASME Code.
- Margin due to flaw size: This margin is generally coupled with the aforementioned margin on K_I. For ASME Code Appendix G calculations for pressure temperature operating curves, an assumed large flaw size of ¼-thickness of the vessel wall is used. In IWB-3611/Appendix A where a detected flaw is being evaluated, the margin on flaw size is a factor of 10 relative to the critical flaw size, which is reflected by the value of √10 that appears in Table 2.

By way of example Figure 8 illustrates the effect of these margin terms on the situations from Figure 5 and Figure 6 where the ASME models are most in need of margin to be conservative.

- The upper graph in Figure 8 shows that a RT_{NDT} margin of +20 °C (approximately the median from Figure 7) plus a K_I margin of √2 is sufficient to make the ASME K_{Ic} model bounding on lower shelf and in transition for most steels. However, a larger K_I margin (=2) would be needed to ensure bounding on the upper

[3] It should be noted that with the exception of Code Case N-749 [4] the ASME Code does not now explicitly consider the area from the upper transition region to the upper shelf. Instead the Code independently assesses cleavage fracture in the transition region using linear elastic fracture mechanics (LEFM), and on the upper shelf using elastic-plastic fracture mechanics (EPFM), in each case with appropriate margin terms.

shelf for high RT_{To} materials. It should be noted that the effectiveness of the Appendix G K_I margins, which are just applied to the K arising due to pressure, are not assessed here. Since these margins apply only to a portion of K, greater values (i.e., greater than 2) would be needed to ensure bounding on the upper shelf.

- The lower graph in Figure 8 shows that a RT_{NDT} margin of +40 °C (higher than any of the values in Figure 7) plus a K_I margin of √2 is sufficient to make the ASME K_{Ia} model bounding on lower shelf and in transition for most steels.

These examples illustrate that in many, but certainly not all, cases combination of the ASME models and these margin terms results in a conservative characterization of K_{Ic} and K_{Ia} relative to data now available. Nevertheless, the degree of conservatism is by no means consistent across the range of conditions found in the operating fleet.

CONCLUSIONS

A. For RT_{NDT}-based Characterizations

For RT_{NDT}-based assessments the comparisons of the ASME model predictions to the data demonstrate the necessity of maintaining the current margins on RT_{NDT} and on K_I to compensate for the inaccuracies of the ASME models. Maintenance of these margins is expected to enable the ASME models to produce conservative characterizations in most cases. However, the information presented herein demonstrates that conservatism cannot be guaranteed in all cases. Additionally, the actual margin achieved by the combination of explicit and implicit margins currently adopted by the Code varies considerably across the fleet, and instances can be found where the actual margin achieved is less than one would wish. In our view, the best remedy to ensure consistent and quantifiable margins is the adoption of a T_o-based assessment strategy. Such a goal has been the focus of Code Cases and various activities within the Code over the past fifteen years. The following section summarizes briefly these past efforts, and goes on to suggest a more integrated approach that could be adopted moving forward.

B. For T_o-based Characterizations

Existing Code activities address some, but not all, of the needed components of a model that is fully consistent with the data and with current-day understandings of the fracture toughness behavior of ferritic steels. These activities, which are in some cases in accord with the data and in other cases are not, are listed in Table 3. To augment these activities and bring them into closer accord with the underlying data, this paper summarizes a model of the fracture toughness behavior across the entire temperature range from lower to upper shelf. This model, which can be based on the information summarized herein, depends only on a value of T_o and on a selected bounding probability value, p, where (for example), p could equal 0.05 as is typical for many engineering applications. Table 4 summarizes the equations, inputs and constants, and limits that fully define this model for calculation of central tendency (median, mean) values while Table 5 summarizes the same information for calculation of a bounding value of fracture toughness. These tables do not present new equations, but rather recast those previously presented in Table 1 in a compact format.

The equations of Table 4 and Table 5 capture the effect of radiation embrittlement (or, equivalently, of T_o) on the interrelationships of K_{Jc}, K_{Ia}, J_{Ic}, and $J_{0.1}$. This feature absent from existing ASME models, and its absence is responsible for many of the inaccuracies of ASME models noted herein. What remains absent from Table 4 and Table 5 are equations to predict the effects of radiation on T_o if this effect is not measured. Various embrittlement trend curves are available for this purpose [29, 31-33] for ASME use in replacing current toughness models the equations given in Table 5 could be expressed as a low probability (p) value (e.g., 5%), with the specific p-value perhaps tied to the loading condition as is now the practice in IWB-3612. The appropriate margins to use with this data-consistent approach, beyond the margin associated with this selection of a p-value, merits further discussion. Reconsidering the types of margins used currently:

Table 3. ASME Code use of models from Table 1.

ID	Summary	Accuracy
N-629 [2] N-631 [3] App. A App. G	Use RT_{To} to index the K_{Ic} and K_{Ia} curves	K_{Ic}: OK in transition. Need margin on lower shelf
		K_{Ia}: inconsistent with the data, but being fixed [34]
N-749 [4]	Defines a temperature (T_c) above which EPFM analysis is needed	The temperature T_c is not a function of T_o, which is not consistent with the data.
Proposed N-830 [35]	Re-defines the K_{Ic} curve as a fixed percentile of the Master Curve in transition and a constant value on lower shelf.	The constant lower shelf value follows current ASME practice but is not consistent with the Master Curve bound and fracture toughness data.

- Margin on T_o: With the elimination of the uncertainty on the unirradiated value of RT_{NDT} (which, as illustrated here, consumed a large part of the existing margin), less margin seems necessary. It is suggested that two factors be considered: the measurement uncertainty on T_o (see [19]), and the uncertainty in the embrittlement shift prediction (see [29, 31-33]). As is current practice a square root sum of squares combination of these two factors can be used. Additionally, should a direct measurement of T_o in the irradiated condition be made then some reduction of these margin terms would be in order.
- Margin on K: The values of K_{Ic} and K_{Ia} on the lower shelf that are exhibited by the data, and are therefore reflected by equations listed in Table 4 and Table 5, are lower than the values predicted by current ASME models. It is recognized that this presents a particular challenge within the ASME Section XI Appendix G context of setting P-T limits for normal operation because a positive head pressure on the pumps needs to be maintained. Figure 8 illustrated that the current ASME models with a √2 margin term on K_I produces K_{Ic} and K_{Ia} values roughly equivalent to a 2.5th percentile curve of the equations listed in Table 5 In view of the added accuracy associated with a To-based approach the use of a bounding p-value and no additional margin on K_I seems appropriate. Should this not produce a sufficiently wide P-T corridor for routine heat-up and cool-down it is suggested that the conservatism inherent to the use of a ¼t flaw in establishing the P-T limits be revisited by the Code.

SUMMARY

In 1972 when ASME adopted the K_{Ic} and K_{Ia} curves and much of the current margin approach, the margins were established based mostly on engineering judgment. Now, ample data exists to build more accurate toughness models and to quantify the amount of margin needed to bound the data; this paper addresses both topics. The models summarized in this paper are based on T_o; they produce safety margins that are both consistent and quantifiable across the fleet, a benefit that cannot be obtained within the current correlative

framework based on RT_{NDT}. Additionally, while the information presented here demonstrates the conservatism of the current RT_{NDT}–based approach in most cases, available data shows it may be non-conservative in some situations. It is suggested that the cognizant ASME Code committees consider these models so that the Code can achieve the benefits made possible by use of current technology and data.

REFERENCES

[1] PVRC Ad Hoc Group on Toughness Requirements, "PVRC Recommendations on Toughness Requirements for Ferritic Materials." Welding Research Council Bulletin No. 175, August 1972.

[2] American Society Of Mechanical Engineers, Use of Fracture Toughness Test Data to Establish Reference Temperature for Pressure Retaining Materials, Section XI, Division 1, ASME Boiler and Pressure Vessel Code Case N-629, ASME, New York (1999).

[3] American Society Of Mechanical Engineers, Use of Fracture Toughness Test Data to Establish Reference Temperature for Pressure Retaining Materials Other than Bolting for Class 1 Vessels, Section III, Division 1, ASME Boiler and Pressure Vessel Code: An American National Standard, Code Case N-631, ASME, New York (1999).

[4] American Society Of Mechanical Engineers, Alternative Acceptance Criteria for Flaws in Ferritic Steel Components Operating in the Upper Shelf Temperature Range, Section XI, Division 1, ASME Boiler and Pressure Vessel Code Case N-749, ASME, New York (2011).

[5] EricksonKirk, M.T., and EricksonKirk, M.A., "Use of a Unified Model for the Fracture Toughness of Ferritic Steels in the Transition and on the Upper Shelf in Fitness-for-Service Assessment and in the Design of Fracture Toughness Experiments," 2006 ASME Pressure Vessel and Piping Conference, PVP2006-ICPVT11-93652.

[6] Williams, P., Dickson, T., and Yin, S., "Fracture Analysis of Vessels – Oak Ridge FAVOR, v12.1, Computer Code: Theory and Implementation of Algorithms, Methods, and Correlations," Oak Ridge National Laboratory Report ORNL/TM-2012/567, United States Nuclear Regulatory Commission ADAMS Accession Number ML13008A014, (2012).

[7] 10 CFR 50.61a, "Alternate fracture toughness requirements for protection against pressurized thermal shock events," http://www.nrc.gov/reading-rm/doc-collections/cfr/part050/part050-0061a.html.

[8] ASME Boiler and Pressure Vessel Code, Rules for Inservice Inspection of Nuclear Power Plants, Section XI, Appendix A., "Analysis of Flaws"

[9] ASME Boiler and Pressure Vessel Code, Rules for Inservice Inspection of Nuclear Power Plants, Section XI, Appendix G., "Fracture Toughness Criteria for Protection against Failure"

[10] ASME NB-2331, 1998 ASME Boiler and Pressure Vessel Code, Rules for Construction of Nuclear Power Plants, Division 1, Subsection NB, Class 1 Components

[11] Kirk, M.T., Stevens, G.L., Erickson, M.A., and Yin, S., "A Proposal for the Maximum K_{Ic} for use in ASME Code Flaw and Fracture Toughness Evaluations," 2011 ASME Pressure Vessel and Piping Conference, PVP2011-57173.

[12] Wallin, K., "The Scatter in K_{Ic} Results," Engineering Fracture Mechanics, 19(6), pp. 1085-1093, 1984.

[13] Wallin, K., "The Size Effect in K_{Ic} Results," Engineering Fracture Mechanics, 22, pp. 149-163, 1985.

Table 4. Equations to estimate central tendency (mean, median) fracture toughness values for ferritic steels, and their variation with temperature.

Toughness	Equations	Eq. #	Inputs and Constants	Limits
Cleavage crack initiation, lower shelf and transition	$K_{Jc} = 30 + 70 \cdot \exp(0.019(T - T_o))$	(4)	T_o measured as per ASTM E1921	$T \le T_{US}$, T_{US} per eq. (11)
Cleavage crack arrest	$T_{KIa} = T_o + 44.97exp[-0.00613T_o]$	(10)	T_o, as above	---
	$K_{Ia} = 30 + 70 \cdot \exp(0.019(T - T_{KIa}))$	(7a)		
Ductile crack initiation on the upper shelf	$T_{US} = 48.843 + 0.7985T_o$	(11)	T_o, as above n, from fit to J-R curve of the form $J = C(\Delta a)^n$ $E = \{207200 - 57.1 \cdot T\}$ $T_{US}^K = T_{US} + 273.15$ $\nu = 0.3$ $C_1 = 1033$ MPa $C_2 = 0.00698$/K $C_3 = 0.000415$/K $\dot{\varepsilon} = 0.0004$/sec	$T > T_{US}$, T_{US} per eq. (11)
	$J_{c(US)} = \{30 + 70 \cdot \exp(0.019(T_{US} - T_o))\}^2 (1 - \upsilon^2)/E$	(8)		
	$\Delta J_{Ic(US)} = 1.75\{C_1 \cdot \exp[-C_2 T_{US}^K + C_3 T_{US}^K \cdot \ln(\dot{\varepsilon})] - 3.325\}$			
	$J_{adj} = J_{c(US)} - \Delta J_{Ic(US)}$			
	$J_{Ic} = 1.75\{C_1 \cdot \exp[-C_2 T_K + C_3 T_K \cdot \ln(\dot{\varepsilon})] - 3.325\} + J_{adj}$			
	$J_{0.1} = J_{Ic} exp(2n)$	(A1)		

Notes: By performing these calculations beginning at the top and moving to the bottom of this table, all variables will be defined in the order that they are needed in later equations.

Table 5. Equations to estimate bounding fracture toughness values for ferritic steels, and their variation with temperature.

Toughness	Equations	Eq. #	Inputs and Constants	Limits
Cleavage crack initiation, lower shelf and transition	$K_{Jc}^{p} = K_{\min} + (K_o - 20)\left\{-\left[\ln(1-p)\right]^{1/4}\right\}$, where $K_o = 31 + 77 \cdot \exp(0.019(T - T_o))$	(5)	T_o measured as per ASTM E1921 p is a selected bounding value (e.g., 0.01, 0.025, 0.05)	$T \le T_{US}$, T_{US} per eq. (11)
Cleavage crack arrest	$T_{KIa} = T_o + 44.97exp[-0.00613T_o]$	(10)	T_o as above	---
	$K_{Ia} = 30 + 70 \cdot \exp(0.019(T - T_{KIa}))$ $K_{Is}^{p} = K_{Is}(1 - 0.18M_p)$	(7a) (7b)	p / M_p: 0.01 / 2.33 0.025 / 1.96 0.05 / 1.64	
Ductile crack initiation on the upper shelf	$T_{US} = 48.843 + 0.7985T_o$	(11)	T_o, as above n, from fit to J-R curve of the form $J = C(\Delta a)^n$ $E = \{207200 - 57.1 \cdot T\}$ $T_{US}^{K} = T_{US} + 273.15$ ν = 0.3 C_1 = 1033 MPa C_2 = 0.00698/K C_3 = 0.000415/K $\dot{\varepsilon}$ = 0.0004/sec	$T > T_{US}$, T_{US} per eq. (11)
	$J_{c(US)} = \{30 + 70 \cdot \exp(0.019(T_{US} - T_o))\}^2 (1 - \upsilon^2)/E$	(8)		
	$\Delta J_{Ic(US)} = 1.75\{C_1 \cdot \exp[-C_2 T_{US}^{K} + C_3 T_{US}^{K} \cdot \ln(\dot{\varepsilon})] - 3.325\}$			
	$J_{adj} = J_{c(US)} - \Delta J_{Ic(US)}$			
	$J_{Ic} = 1.75\{C_1 \cdot \exp[-C_2 T_K + C_3 T_K \cdot \ln(\dot{\varepsilon})] - 3.325\} + J_{adj}$			
	$\sigma_{\Delta J_{Ic}} = A \cdot e^{(B \cdot \hat{T})}$ where $\hat{T} = T - 288^{\circ}\mathrm{C}$ $A = 9.03 \cdot e^{(1.12 \cdot P)}$ $B = MIN\{0, 0.0009P - 0.0045\}$ $P = MIN\{1, MAX[0, MIN(P_1, P_2)]\}$ $P_1 = \frac{J_{Ic(288)}}{120} - 0.46$ $P_2 = \frac{J_{Ic(288)}}{800} + 0.51$	(9)		
	$J_{Ic}^{p} = J_{Ic} - \sigma_{\Delta J_{Ic}} M_p$	(8-9)	M_p as above	
	$J_{0.1}^{p} = J_{Ic}^{p} exp(2n)$	(A1)	---	

Notes: By performing these calculations beginning at the top and moving to the bottom of this table, all variables will be defined in the order that they are needed in later equations.

[14] Wallin, K., "Irradiation Damage Effects on the Fracture Toughness Transition Curve Shape for Reactor Vessel Steels," *Int. J. Pres. Ves. & Piping*, 55, pp. 61-79, 1993

[15] EricksonNatishan, MarjorieAnn, "Establishing a Physically Based, Predictive Model for Fracture Toughness Transition Behavior of Ferritic Steels (MRP-53)": Materials Reliability Program (MRP), EPRI, Palo Alto, CA:2001. 1003077.

[16] Kirk, M., Lott, R., Kim, C., and Server, W., "Empirical Validation Of The Master Curve For Irradiated And Unirradiated Reactor Pressure Vessel Steels," Proceedings of the 1998 ASME/JSME Pressure Vessel and Piping Symposium, July 26-30, 1998, San Diego, California, USA.

[17] IAEA TRS-429, "Guidelines for application of the master curve approach to reactor pressure vessel integrity in nuclear power plants," International Atomic Energy Agency, Vienna Austria, 2005.

[18] Wallin, K., "Application of Master Curve to Highly Irradiated RPV Steels," Presentation to the LONGLIFE Final Workshop, 15-16 January 2014, Dresden Germany, http://projects.tecnatom.es/webaccess/LONGLIFE/.

[19] ASTM E1921-02, "Test Method for Determination of Reference Temperature, T_o, for Ferritic Steels in the Transition Range," ASTM, 2002.

[20] Wallin, K., and Rintamaa, R., "Master Curve Based Correlation between Static Initiation Toughness K_{Ic} and Crack Arrest Toughness K_{Ia}," Proceedings of the 24th MPA-Seminar, Stuttgart, October 8 and 9, 1998.

[21] Kirk, M. T., Natishan, M. E., and Wagenhofer, M., "A Physics-Based Model for the Crack Arrest Toughness of Ferritic Steels," *Fatigue and Fracture Mechanics, 33rd Volume, ASTM STP-1417*, W. G. Reuter, and R. S. Piascik,

Eds., American Society for Testing and Materials, West Conshohocken, PA, 2002.

[22] EricksonKirk, Marjorie and EricksonKirk, Mark, "An Upper-Shelf Fracture Toughness Master Curve for Ferritic Steels," Submitted to *International Journal of Pressure Vessels and Piping*, **83** (2006) 571–583

[23] *Materials Reliability Program: Implementation Strategy for Master Curve Reference Temperature, T_o (MRP-101),* EPRI, Palo Alto, CA, and U.S. Department of Energy, Washington, DC: 2004. 1009543.

[24] EricksonKirk, Marjorie and EricksonKirk, Mark, "The Relationship between the Transition and Upper Shelf Fracture Toughness of Ferritic Steels." *Fatigue Fract Engng Mater Struct* **29**, 672–684 (2006).

[25] 10 CFR 50.61, "Fracture toughness requirements for protection against pressurized thermal shock events," http://www.nrc.gov/reading-rm/doc-collections/cfr/part050/part050-0061.html.

[26] *Application of Master Curve Fracture Toughness Methodology for Ferritic Steels* (PWRMRP-01): PWR Materials Reliability Project (PWRMRP); EPRI, Palo Alto, CA: 1999. TR-108930.

[27] Wallin, K., and Rintamaa, R., "Statistical Definition of the ASME Reference Curves," Proceedings of the MPA Seminar, University of Stuttgart, Germany, October 1997.

[28] B. Houssin, R. Langer, D. Lidbury, T. Planman and K. Wallin, "Unified reference fracture toughness design curves for RPV steels - Final Report", CEC-DG XI Contract B7-5200/97/000809/MAR/C2, EE/S.01.0163.Rev. B 2001.

[29] U.S. Nuclear Regulatory Commission Regulatory Guide 1.99 Radiation Embrittlement of Reactor Vessel Materials, May1988, http://pbadupws.nrc.gov/docs/ML0037/ML003740284.pdf

[30] Nuclear Regulatory Commission Reactor Vessel Integrity Database, Version 2.1.1, July 6, 2000.

[31] Charpy Embrittlement Correlations—Status of Combined Mechanistic and Statistical Bases for U.S. RPV Steels (MRP-45): PWR Materials Reliability Program (PWRMRP), EPRI, Palo Alto, CA: 2001. 1000705.

[32] "Developing an Embrittlement Trend Curve Using the Charpy "Master Curve" Transition Reference Temperature," Reliability Program (MRP-289), EPRI, Palo Alto, CA: 2011. 1020703.

[33] Kirk, Mark, "A Wide-Range Embrittlement Trend Curve for Western Reactor Pressure Vessel Steels," Effects of Radiation on Nuclear Materials on June 15, 2011 in Anaheim, CA; STP 1547, Takuya Yamamoto, Guest Editor., pp. 1–32, doi:10.1520/STP103999, ASTM International, West Conshohocken, PA 2012.

[34] Kirk, M., Hein, H., Erickson, M., Server, W., and Stevens, G., "Fracture-Toughness based Transition Index Temperatures for use in the ASME Code with the Crack Arrest (K_{Ia}) Curve," ASME Pressure Vessel and Piping Meeting 2014, PVP2014-28311.

[35] Proposed Code Case N-830 (BC 09-182), Direct Use of Master Fracture Toughness Curve for Pressure Retaining Materials for Vessels of a Section XI, Division 1, Class.

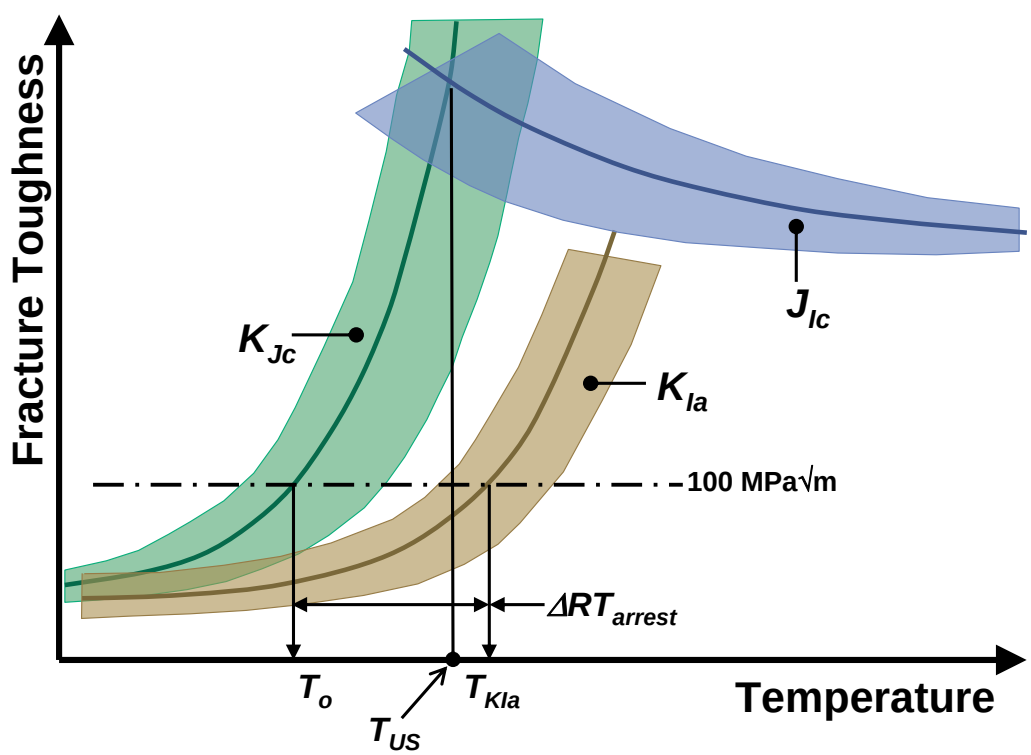

Figure 1. Illustration of the variables used by the models in Table 1 to describe the fracture toughness of ferritic steels.

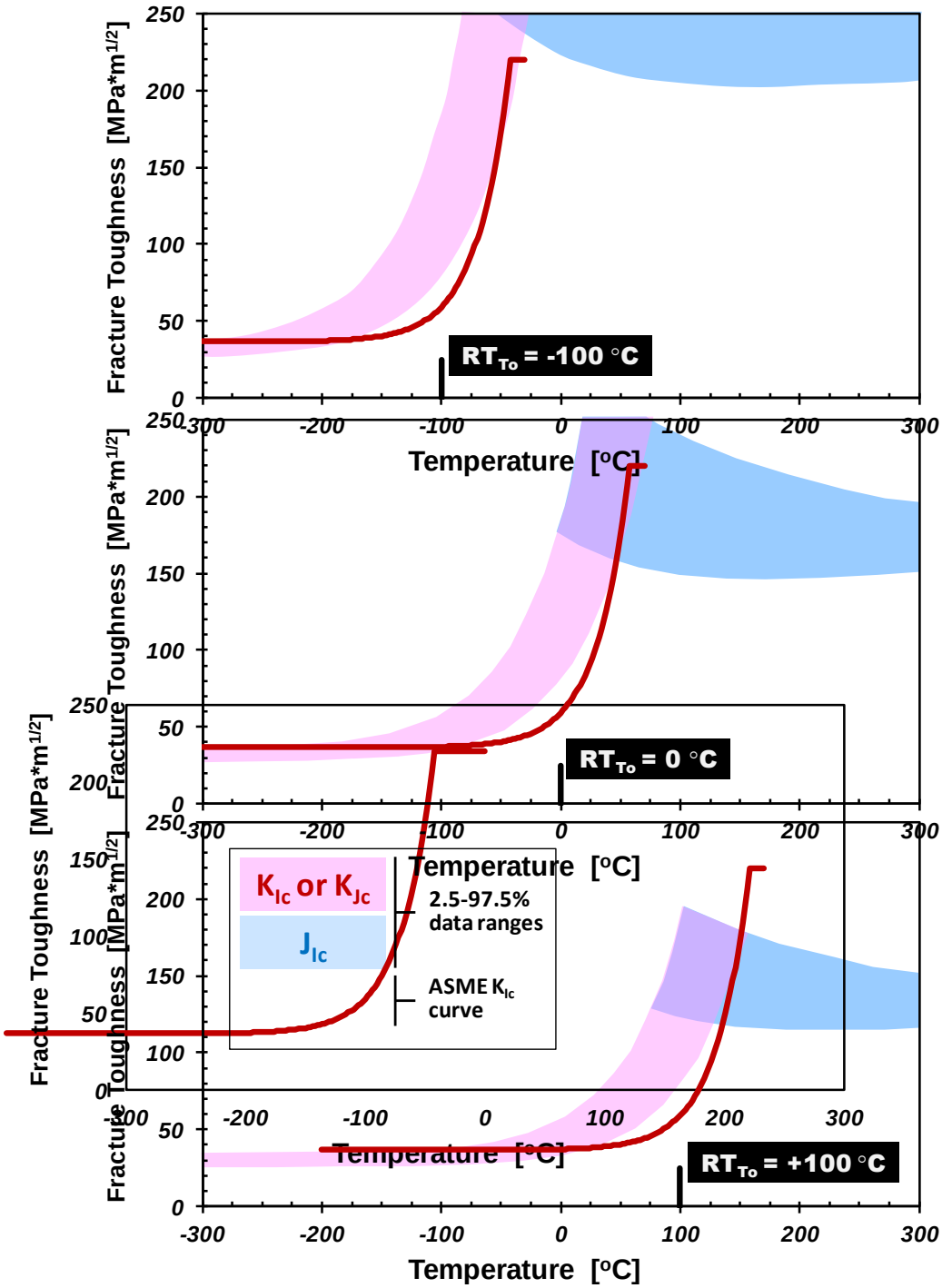

Figure 2. Comparison of ASME K_{Ic} curve (truncated at the *de facto* limit of 220 MPa√m) to data-based models of K_{Ic} / K_{Jc} (pink) and J_{Ic} (blue). The shaded regions depict the 97.5% / 2.5% confidence bounds for the data-based models. Within the overlap of the shaded regions there is competition between cleavage and ductile fracture.

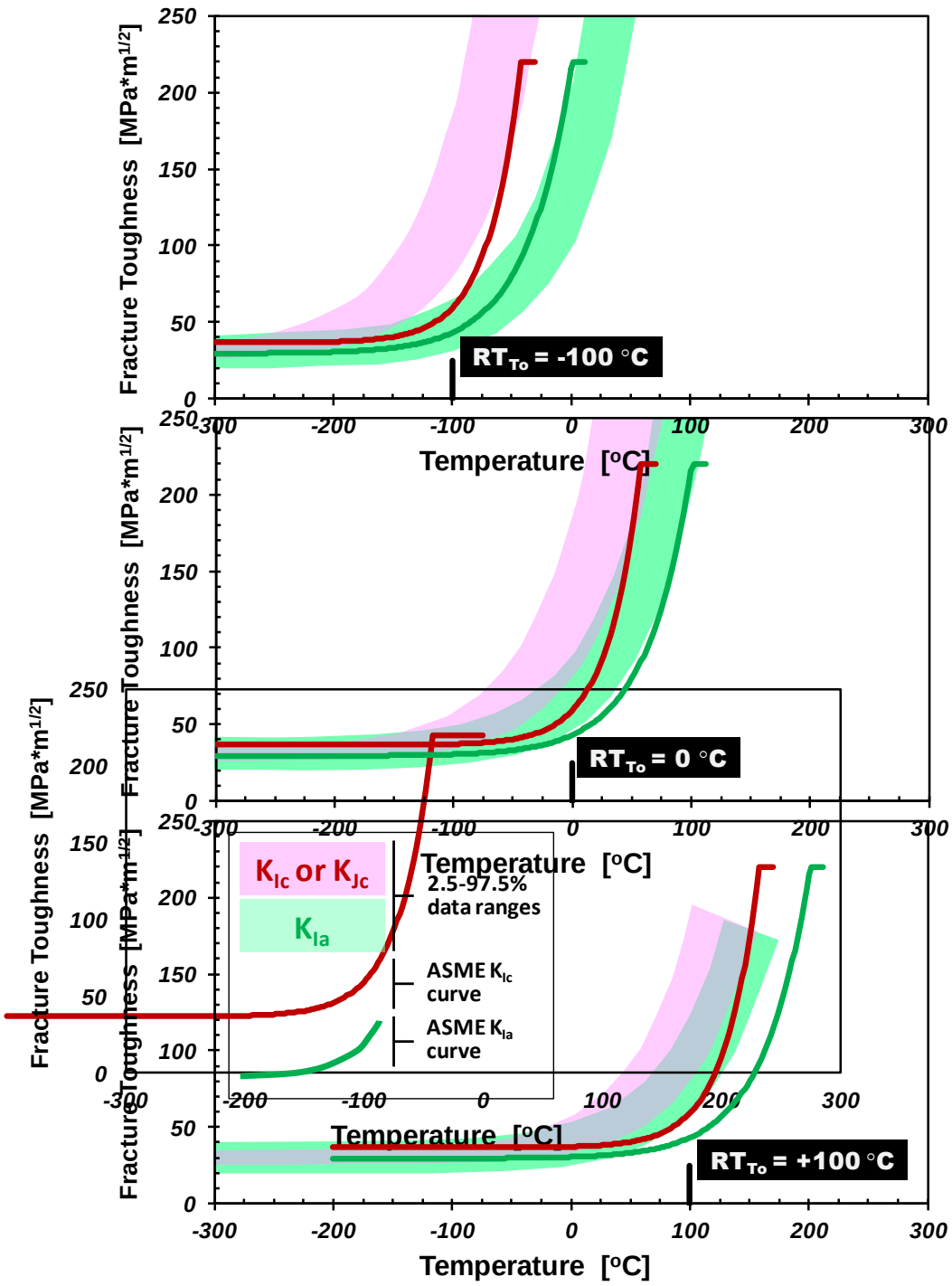

Figure 3. Comparison of ASME K_{Ic} and K_{Ia} curves (truncated at the *de facto* limit of 220 MPa√m) to data-based models of K_{Ic} / K_{Jc} (pink) and K_{Ia} (green). The shaded regions depict the 97.5% / 2.5% confidence bounds for the data-based models.

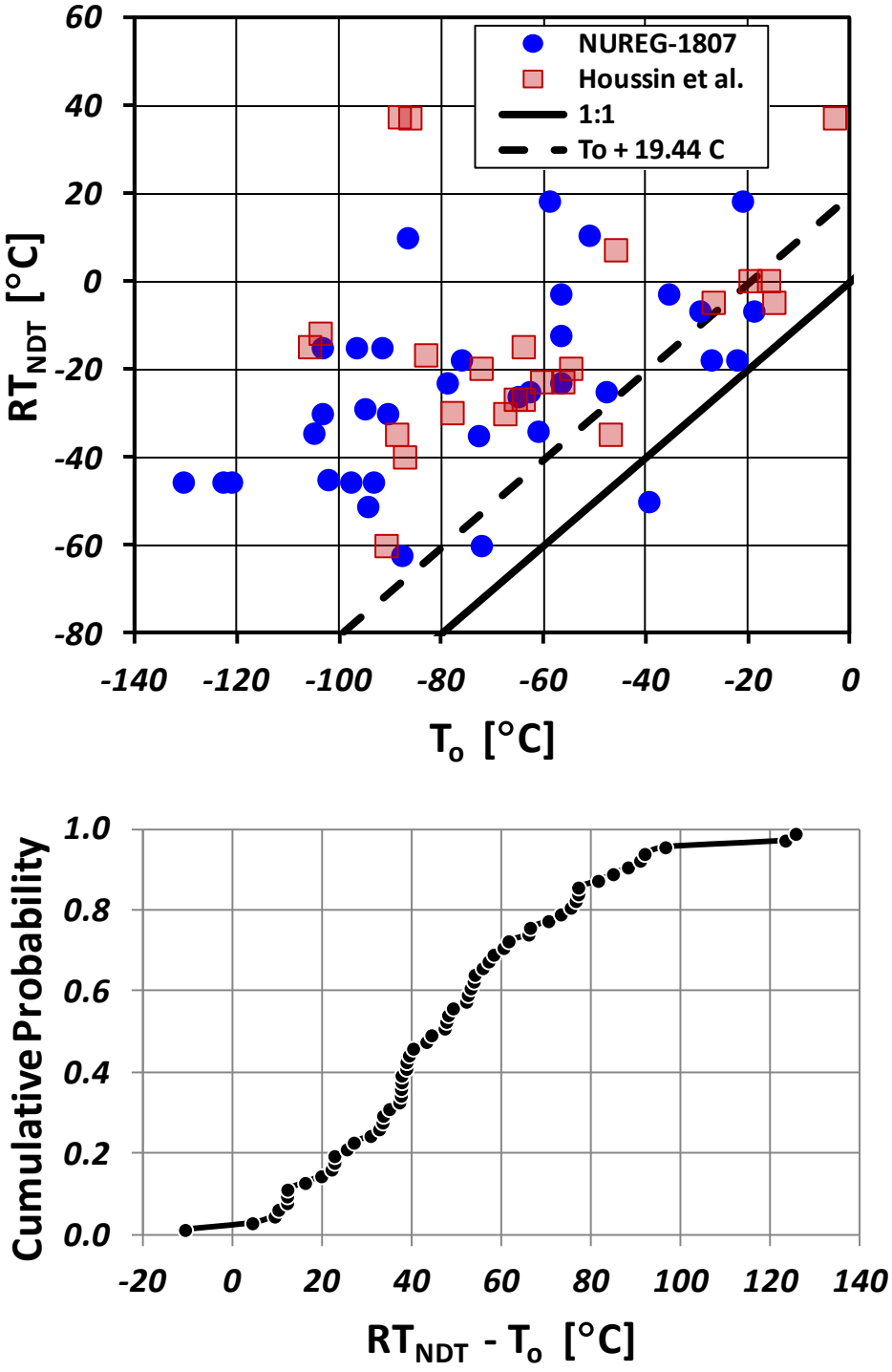

Figure 4. Combination of data from [6] and [28] where measurements of RT_{NDT} and T_o are available for the same materials to illustrate the considerable range by which RT_{NDT} can exceed T_o.

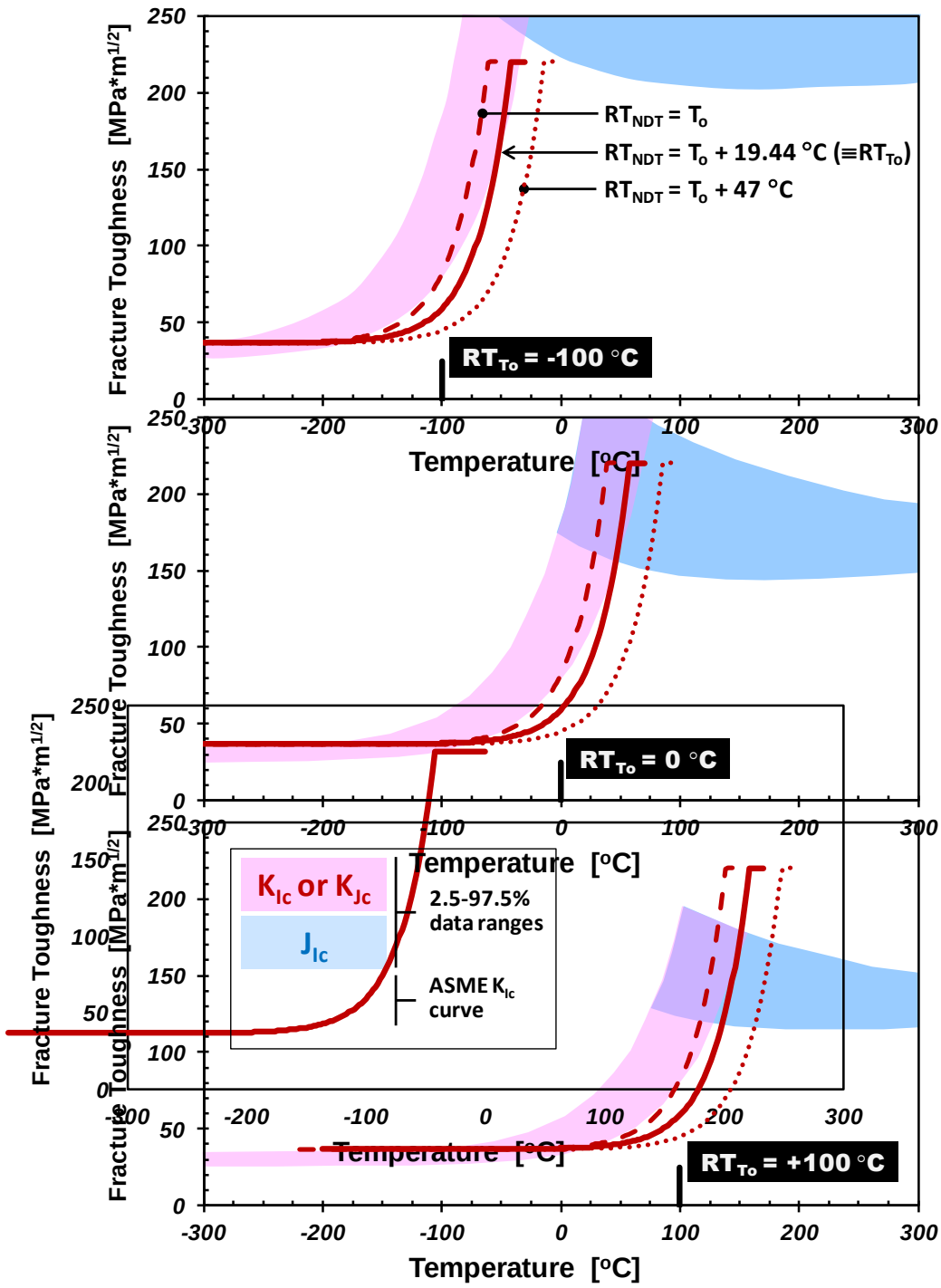

Figure 5. Comparison of ASME K_{Ic} curve (truncated at the *de facto* limit of 220 MPa√m) to data-based models of K_{Ic} / K_{Jc} (pink) and J_{Ic} (blue). The shaded regions depict the 97.5% / 2.5% confidence bounds for the data-based models. The ASME K_{Ic} curve is shown for various temperature differentials between T_o and RT_{NDT}.

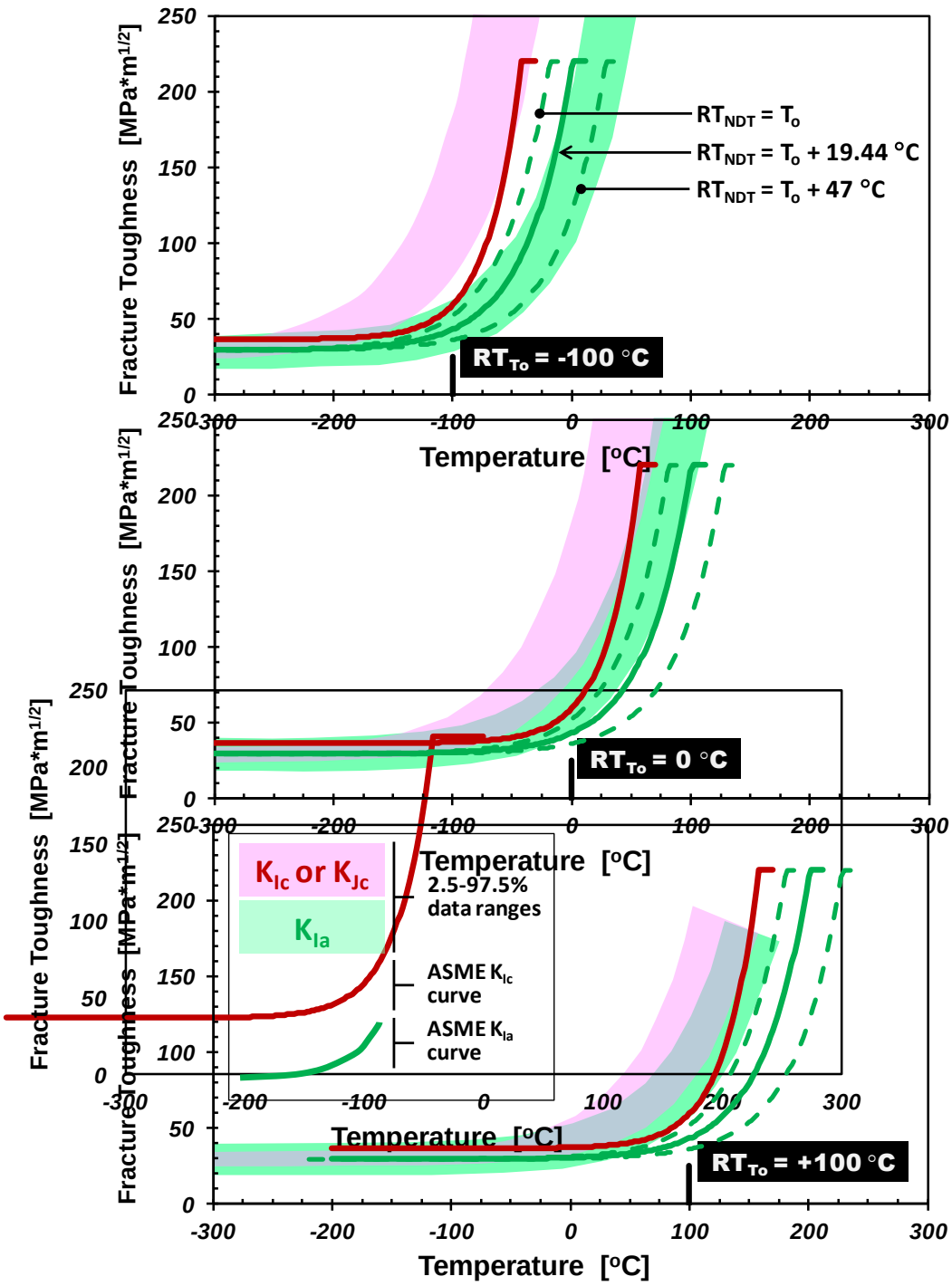

Figure 6. Comparison of ASME K_{Ia} curve (truncated at the *de facto* limit of 220 MPa√m) to data-based models of K_{Ic} / K_{Jc} (pink) and K_{Ia} (green). The shaded regions depict the 97.5% / 2.5% confidence bounds for the data-based models. The ASME K_{Ia} curve is shown for various temperature differentials between T_o and RT_{NDT}.

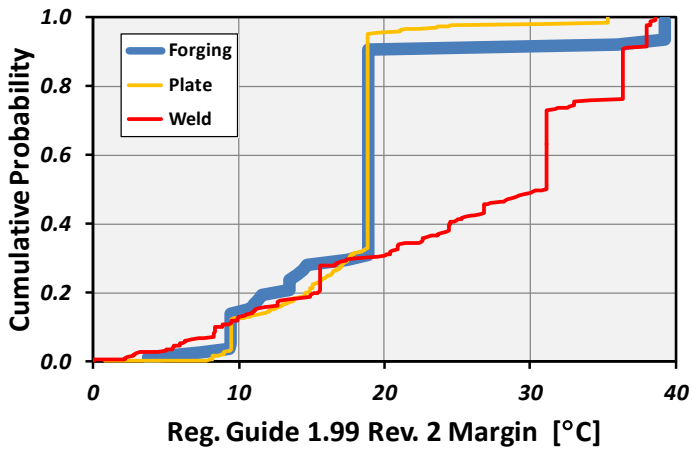

Figure 7. Values of RT_{NDT} margin reported in RVID2 [30].

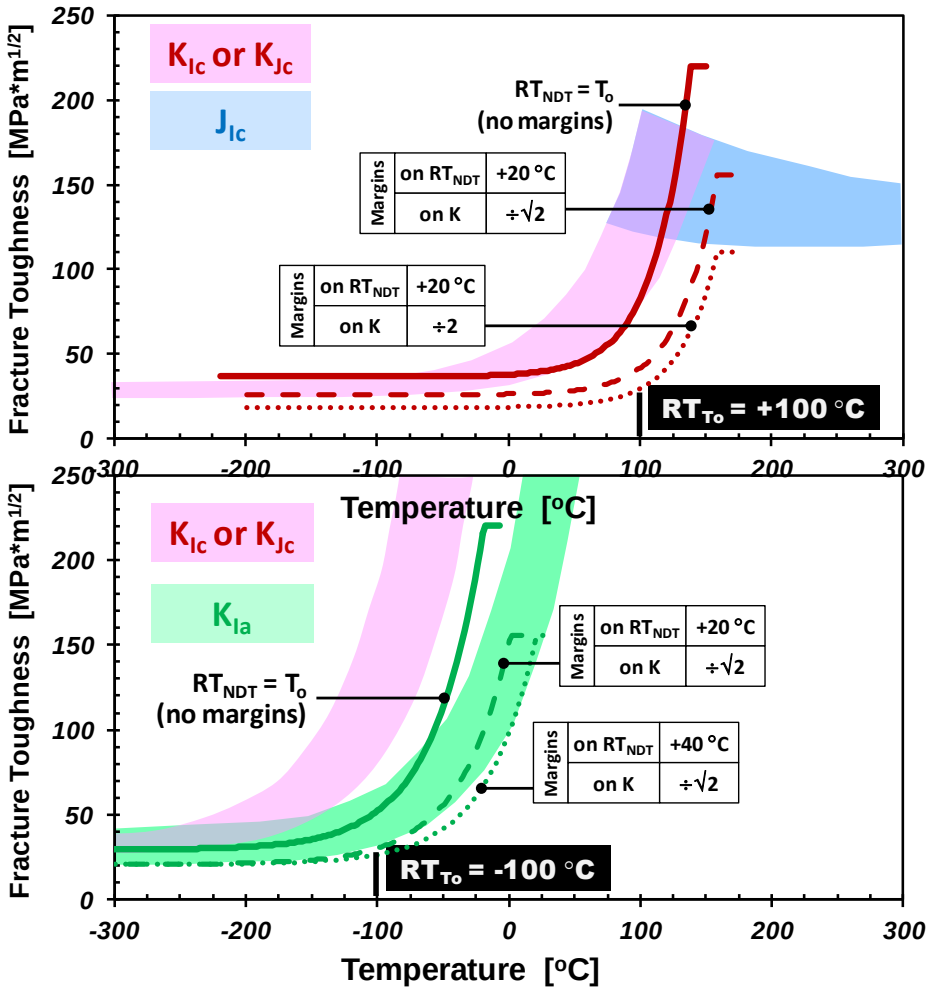

Figure 8. Comparison of ASME models (curves) with various margin terms applied to data-based models of K_{Ic} / K_{Jc} (pink), J_{Ic} (blue), and K_{Ia} (green). The ASME models are all truncated at the *de facto* limit of 220 MPa√m. The shaded regions depict the 97.5% / 2.5% confidence bounds for the data-based models.

APPENDIX: RELATIONSHIP BETWEEN $J_{0.1}$ AND J_{Ic}

Background

Nonmandatory Appendix K of the ASME Code, *"Assessment of Reactor Vessels with Low Upper Shelf Charpy Impact Energy Levels,"* [A1] adopts an elastic-plastic fracture mechanics assessment method based on the *J-R* curve. Appendix K does not use J_{Ic} as a parameter characterizing ductile crack initiation, but rather adopts the parameter $J_{0.1}$, with the subscript denoting that this is the value of *J* at 0.1 inches (2.5 mm) of stable ductile crack growth. J_{Ic} is determined at the onset of ductile crack growth [A2]; since the *J-R* curve is rapidly increasing for most reactor materials at loading levels around J_{Ic} values of J_{Ic} can exhibit considerable scatter. The ASME Code therefore adopted $J_{0.1}$ as an engineering measure of ductile crack initiation; it generally exhibits less scatter than does J_{Ic}.

$J_{0.1}$ Model

In NUREG/CR-5729 Eason et al. assembled from the literature a considerable collection (over 500 specimens) of *J-R* curve data, including both unirradiated and unirradiated RPV materials, welds as well as base metal, and also nuclear grade piping materials [A3]. Figure A1 shows all of these data, plotted as a function of temperature, where upper shelf is characterized using both J_{Ic} and $J_{0.1}$. As previously reported by Kirk et al. [A4], the J_{Ic} characterization demonstrates that in virtually every case ASME's *de facto* upper limit on K_{Ic} of 220 MPa√m is non-conservative. Conversely, the $J_{0.1}$ characterization of upper shelf shows that for many, but certainly not all, materials ASME's *de facto* upper limit on K_{Ic} of 220 MPa√m is appropriate or conservative.

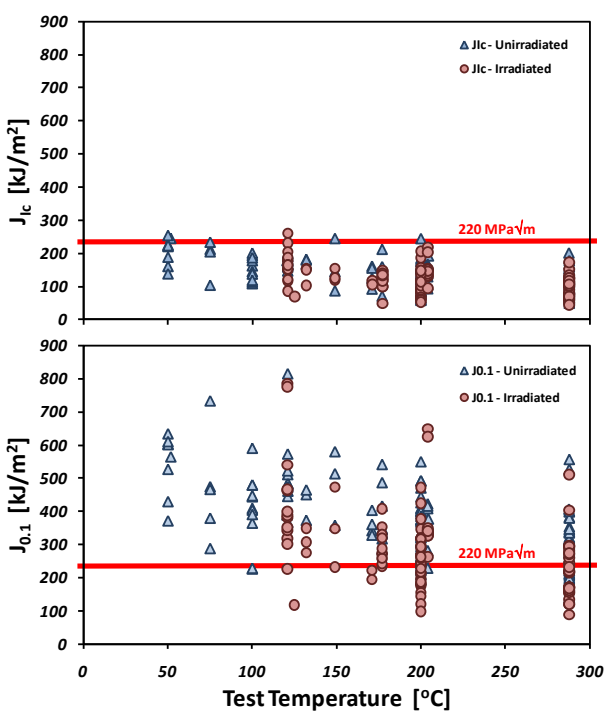

Figure A1. Data from [ref] plotted in terms of both J_{Ic} (top) and $J_{0.1}$ (bottom). The de facto ASME limit on K_{Ic} of 220 MPa√m, converted to J units, is shown on each graph.

The *J-R* curve data in NUREG/CR-5729 exhibit a clear relationship between the ratio of $J_{0.1}/J_{Ic}$ and the J-R curve exponent *n* (see Figure A2), as follows:

$$\frac{J_{0.1}}{J_{Ic}} = exp(2n) \tag{A1}$$

This relationship can be used to convert the J_{Ic}-based K_{Ic} limit proposed by Kirk et al. [A4]:

$$K_{Ic}^{LIMIT} = 151.771 \cdot exp(-0.00271 \cdot RT_{To}) \tag{A2}$$

to one based on $J_{0.1}$:

$$K_{Ic}^{LIMIT} = \{151.771 \cdot exp(-0.00271 \cdot RT_{To})\}\sqrt{exp(2n)} \tag{A3}$$

Figure A3 compares the limit of eqn. (A2) to that of eqn. (A3), and to the *de facto* ASME limit of 220 MPa√m for different values of the *J-R* curve exponent *n*. For high values of *n* and low values the RT_{To} reference temperature the ASME limit is appropriate or conservative. However, in view of the tendency for irradiation damage to increase RT_{To} and also reduce *n*, it seems that the continued use of a 220 MPa√m upper limit on K_I be re-examined. Figure A4 provides an illustrative example of the elevation of $J_{0.1}$ above J_{Ic} for two different values of *n*.

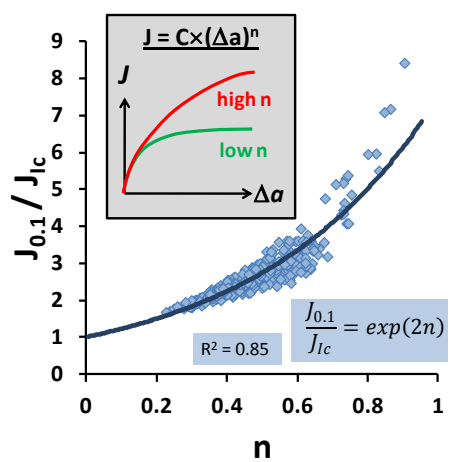

Figure A2. Data from [ref] showing a clear relationship between the ratio $J_{0.1}/J_{Ic}$ (top) and the *J-R* curve exponent *n*.

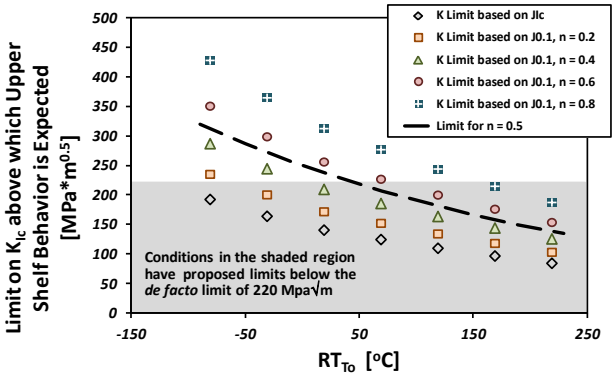

Figure A3. Illustration of the effect of *J-R* curve exponent *n* on the K_{Ic} upper shelf limit supported by upper shelf toughness as characterized by $J_{0.1}$. The K_{Ic} limit based on J_{Ic} was proposed in [A4].

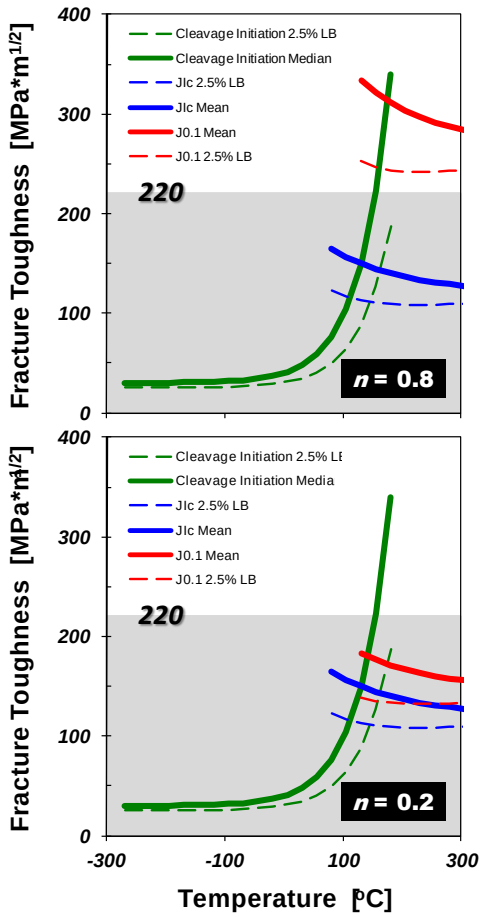

Figure A4. Illustration of the effect of *J-R* curve exponent *n* (*n*=0.8 top, *n*=0.2 bottom) on the magnitude of upper shelf toughness characterized by $J_{0.1}$ for a material having RT_{To} = 102 °C.

References

[A1] ASME Boiler and Pressure Vessel Code, Rules for Inservice Inspection of Nuclear Power Plants, Section XI, Appendix G., "Assessment of Reactor Vessels with low Upper Shelf Charpy Impact Energy Levels"

[A2] ASTM E1820, *Standard Test Method for Measurement of Fracture Toughness*, ASTM International, West Conshohocken, Pennsylvania, USA.

[A3] Eason, E.D., Wright, J.E., and Nelson, E.E., "Multivariable Modeling of Pressure Vessel and Piping J-R Data," NUREG/CR-5729, United States Nuclear Regulatory Commission, 1991.

[A4] Kirk, M.T., Stevens, G.L., Erickson, M.A., and Yin, S., "A Proposal for the Maximum K_{Ic} for use in ASME Code Flaw and Fracture Toughness Evaluations," 2011 ASME Pressure Vessel and Piping Conference, PVP2011-57173.